Nanosecond pulsed laser irradiation of titanium in acetone: the effects of coating film structures on the hydrogen absorption properties

Yuki Nakagawa[a*], Genki Sugimoto[b], Tamaki Shibayama[a]

[a] Faculty of Engineering, Hokkaido University, N-13, W-8, Sapporo 060-8628, Japan

[b] Graduate School of Engineering, Hokkaido University, N-13, W-8, Sapporo 060-8628, Japan

* Corresponding author. Tel.: +81 11 706 7134

E-mail address: y-nakagawa@eng.hokudai.ac.jp (Y. Nakagawa)

ABSTRACT

Pulsed laser irradiation was performed on titanium in acetone and then the hydrogen storage properties were investigated under a hydrogen atmosphere. TiO_xC_y films were formed by the irradiation of Ti powders with a fluence of 0.36 J cm^{-2}. The irradiation increased the hydrogen absorption temperatures. Thus, the TiO_xC_y films showed a specific kind of hydrogen barrier effect. Irradiation with a fluence of 0.36 J cm^{-2} was performed to coat the Ti plate. Although the TiO_xC_y films formed on the surface, the amount of hydrogen absorption increased compared with the non-irradiated plate because of the change in surface chemical bonding states and high porosity of the films due to the irradiation. The phases generated by irradiation were controlled by the laser fluence. With a low fluence of 0.17 J cm^{-2}, TiO_2 films were formed instead of TiO_xC_y films, and these dense films showed better hydrogen barrier effects than the non-irradiated plate.

Keywords: Titanium; Nd:YAG laser; hydrogen barrier coating; hydrogen absorption; titanium oxycarbide; titanium oxide

1. Introduction

Titanium is an excellent material for hydrogen capture because of its low ΔH_{abs} value (−142 kJ mol^{-1} H_2), which means that its H_2 equilibrium pressure at room temperature is low [1]. However, hydrogen absorption with Ti requires thermal activation at a temperature above ~400 °C. Therefore, improved absorption kinetics are needed for practical applications. The role of surface oxide layers in the hydrogen absorption properties of Ti has been investigated. Hirooka *et al.* suggested that the absorption process may be affected by the surface oxide layers, whereas the desorption process is probably controlled by the hydrogen diffusion in Ti [2]. Hadjixenophontos *et al.* showed that the rate-limiting factor for hydrogen absorption is the transport of hydrogen atoms through the oxide layers rather than the splitting of H_2 molecules at the oxide surface [3]. Shinzato *et al.* reported that Ti without surface oxide layers can absorb hydrogen even at room temperature [4]. However, Ti generates surface oxide layers even in a glovebox with oxygen and water levels of several ppm; thus, the absorption temperature was increased with time in the glovebox [4]. In this way, the kinetic barrier effects of the surface oxide layers are significant. To modify the surface oxide layers, mechanical milling of Ti powders with acetone [5] or layered solid materials (graphite [5] and hexagonal boron nitride [6]) is an effective method. In addition, Ti can absorb hydrogen even at room temperature during self-shearing reactive milling under a hydrogen atmosphere [7]. However, there are few studies on other surface modification methods besides milling that affect the hydrogen absorption properties of Ti. Kondo *et al.* achieved enrichment of Pd on the surface of Ti–Pd alloys by H_2O_2 immersion, which resulted in fast hydrogenation of Ti [8]. Although the utilization of Pd is effective for selective hydrogen permeation, low-cost surface modification methods would also be required. From a different point of view, for the application of titanium and its alloys in structural materials, a hydrogen barrier coating is required to prevent hydrogen intake–induced embrittlement [9–11]. Thermal spraying [12], enamel coating [13], and laser carburization using carbon paste [14] have been performed in previous studies.

In this study, the effects of surface coating using nanosecond pulsed laser irradiation on the hydrogen absorption properties of Ti were investigated. A facile method for the irradiation of titanium using a pulsed laser and acetone solvent was performed. After pulsed laser coating, the hydrogen absorption temperatures were analyzed. If hydrogen absorption temperatures are decreased by coatings, this would be useful for developing excellent hydrogen permeation layers for Ti as a hydrogen storage metal. Increasing hydrogen absorption temperatures by the application

of coatings, would be helpful in developing superior hydrogen barrier coatings for Ti as a structural material. The formation of titanium carbide nanoparticles by laser ablation of Ti targets in organic solvents has been reported [15,16]. Also, irradiation below the ablation threshold in a liquid can cause pulsed laser melting and various crystalline spherical submicron particles can be formed [17]. In this study, irradiation in organic solvents with a relatively low fluence of several hundred mJ cm^{-2} per pulse was applied.

2. Experimental

2.1 Sample Synthesis

Ti powder (99.98%, ≤45 μm, Nilaco Corporation, Tokyo, Japan), polycrystalline Ti plates (99.5%, 0.3 mm thick, Nilaco Corporation, Tokyo, Japan), and acetone (Specification Assay ≥99.5%, FUJIFILM Wako Pure Chemical Corporation, Osaka, Japan) were purchased and used in this study. The samples were irradiated in acetone using a nanosecond pulsed Q-switched Nd:YAG laser (Inlite II, Continuum, USA) with a wavelength of 532 nm, pulse width of 5–7 ns, and repetition rate of 20 Hz.

Fig. 1 shows the experimental setups for laser irradiation. Fig. 1(a) shows the setup for the powders. ~80 mg Ti powder and a stirring bar were put in a quartz screw vial with a capacity of 5 ml, and the vial was filled with acetone in an Ar-filled glovebox. Then, the closed vial was taken out of the glovebox and laser irradiation was performed in air. The sample powders were stirred during irradiation and no collective lens was used. The laser beam diameter was 5.5 mm and the laser fluence was 0.36 J cm^{-2}. After irradiation, the closed vial was put in the glovebox and the cap was opened to allow the acetone to evaporate overnight. The irradiated number of pulses were 6000 and 54,000 pulses for the powder samples. For irradiation of the Ti plates, hydrogen barrier effects were examined by comparing the two laser fluences of 0.36 J cm^{-2} or 0.17 J cm^{-2}. The number of pulses for Ti plate was fixed to 18,000 pulses. The Ti powders irradiated with 54,000 pulses showed an insufficient hydrogen barrier effects as shown in Fig. 3(f), thus the number of pulses smaller than 54,000 pulses were selected for the irradiation of Ti plates. The plate sample treatment was performed in air. First, Ti plates of dimensions 4 mm × 4 mm × 0.30 mm were prepared using an Isomet low speed saw (Buehler, Illinois, USA). One of the Ti plates was polished with #600, #800, and #1000 water-resistant polishing paper. After single-side polishing, the plate was ultrasonically cleaned in acetone for 10 min. Each Ti plate (unpolished and polished) was put

in a quartz screw vial, which was filled with acetone. As shown in Fig. 1(b), the reflected laser was directed toward the Ti plate in acetone. The laser beam diameter was 5.5 mm, the same as that used for irradiation of the powders. Laser irradiation of the Ti plates was performed on both the front and back sides, but not on the end faces. To irradiate the sample evenly, the sample position was adjusted manually during irradiation. After irradiation, the Ti plate was dried in air and then stored in a desiccator decompressed with a rotary pump.

2.2 Characterization

The crystalline phases were characterized using an X-ray diffractometer with Cu Kα radiation (XRD, MiniFlex, Rigaku, Tokyo, Japan). The sample morphologies were observed using a scanning electron microscope (SEM, JSM-7001FA, JEOL, Tokyo, Japan) with an acceleration voltage of 15 kV. The chemical bonding states of the Ti plates were investigated using a confocal Raman microscope (XploRA, Horiba, Kyoto, Japan) with a laser wavelength of 532 nm in conjunction with a grating having 2400 grooves/nm. X-ray photoelectron spectrometer (XPS, JPS-9200, JEOL, Tokyo, Japan) was used to analyze the chemical bonding states of Ti plate surfaces. Mg Kα radiation was used for the experiment. The samples were analyzed by some experiments in air (Raman microscope and SEM), and then the XPS analysis was performed. The base pressure during spectra acquisition was better than 5.0×10^{-6} Pa achieved by turbomolecular pump. The size of sample analyzed area was 3 mm in diameter and the electron emission angle was 0°. Sputter cleaning or charge neutralizer was not used during the analysis. The binding energy values were calibrated by using the work function method [18]. The work function of TiO_2 was reported to be 4.64 eV [19], therefore the binding energy of C 1s peak was calibrated at 284.94 eV in this work. The hydrogen absorption temperatures were evaluated using a pressure–composition–temperature (PCT) apparatus (Suzuki Shokan, Tokyo, Japan). For the hydrogen absorption tests of the Ti powders, activation treatment (one cycle of hydrogen absorption and desorption) was performed, and then hydrogen reabsorption (a second hydrogen absorption) tests were conducted. For the activation treatment, a hydrogen pressure of ~0.3 MPa was introduced in the PCT cell at room temperature, and then the cell was heated to 580 °C at a heating rate of 10 °C min^{-1}. Then, hydrogen was desorbed at 580 °C under a dynamic vacuum for 4 h. The activation conditions were based on those used in a previous study [6]. For the hydrogen absorption tests of the Ti plates, a hydrogen pressure of ~0.3 MPa was introduced in the cell and the cell was heated up to 580 °C at

a heating rate of 10 °C min^{-1}. The hydrogen absorption test of the polished Ti plate was conducted immediately after the polishing treatment.

3. Results and discussion

3.1 Hydrogen absorption properties of Ti powder

Fig. 2 shows the XRD profiles and SEM images of the pristine Ti powder and laser-irradiated powders. As shown in Fig. 2(a), the Ti powders irradiated with 6000 pulses and 54,000 pulses showed peaks corresponding to hexagonal Ti. In addition, Ti powders irradiated with 54,000 pulses showed broad peaks corresponding to the TiC phase. The crystallite size of TiC estimated by Sherrer equation was in the range of 12-15 nm. The background peaks originate from the grease and polyimide films that are used to avoid contact with air. As shown in the SEM images and EDS spectra in Fig. 2(b)–2(d), enrichment of carbon was observed as the number of pulses increased. The existence of a slight amount of carbon in the unirradiated Ti powder in Fig. 2(b) would be due to a residual gas contamination in the chamber atmosphere. The particle morphology changed with the heat effects of YAG laser irradiation. Both irradiated powders showed melting surface morphologies and several voids appeared on the surface. In the powders irradiated with 54,000 pulses, some spherical-like particles were observed on the surface, as shown in spot E in Fig. 2(d), and the amount of carbon was particularly high in such areas. In addition, a small amount of oxygen was detected from the EDS in Fig. 2(c) and 2(d). Thus, with a fluence of 0.36 J cm^{-2}, laser irradiation in acetone introduced a TiO_xC_y coating. From XRD, TiC phase was observed for the powders irradiated with 54,000 pulses. Thus, the composition of TiO_xC_y would change toward the stoichiometric TiC phase as the number of pulses increased (The process is discussed in Section 3.2). The hydrogen absorption properties of these Ti powders are shown in Fig. 3. The left and right vertical axes show the hydrogen pressure and temperature, respectively. As shown in Fig. 3(a), 3(c), and 3(e), the hydrogen absorption temperature of Ti was slightly increased by the irradiation. Although the pristine Ti powder absorbed hydrogen at ~404 °C with fast kinetics, the irradiated samples absorbed at ~440 °C with slow kinetics. This is also confirmed in the temperature profiles, where a temperature rise from hydrogen absorption is clearly observed for the pristine powder, but not for the irradiated powders. The hydrogen absorption temperature of the pristine Ti powder after the activation treatment decreased at ~167 °C. A significant decrease of absorption temperature of Ti after activation was also observed in previous studies, probably

because of the reduction of TiO_2 surfaces by the H_2 atmosphere at high temperature [20]. However, the laser-irradiated powders showed high absorption temperatures above 260 °C after activation, which indicates that the TiO_xC_y coating would have some hydrogen barrier effects. Previous studies showed that mechanical milling of Ti with a small amount of acetone led to hydrogen absorption at ~40 °C immediately after sample preparation, but high reactivity to H_2 was lost after several days in a glovebox [5]. The results from this milling method suggest the formation of a non-stoichiometric TiC_x phase. Thus, non-equilibrium phase formation from mechanical milling could generate hydrogen permeation films on the surface. It is also reported from density functional theory simulations that the energy barriers for hydrogen diffusion in TiC_x drop with a low value of x [21,22]. However, a TiO_xC_y or TiC phase was formed with the laser irradiation in this study, which causes the hydrogen barrier effects. Hydrogen absorption proceeded through two steps as shown in Fig. 3(f). A slight absorption at 262 °C suggested that a small amount of non-stoichiometric TiC_x may be formed by the number of pulses increases, and this phase may absorb hydrogen. Details of this phenomenon should be investigated in future study.

3.2 Hydrogen absorption properties of Ti plate

Since hydrogen barrier effects were observed for the powder samples in Section 3.1, laser irradiation was also performed on Ti plates, whose hydrogen absorption temperatures would be higher than those of the powders. Fig. 4 shows the hydrogen absorption properties of Ti plates. As shown in Fig. 4(a), an unpolished Ti plate absorbed a small amount of hydrogen above 500 °C. However, a Ti plate polished on one side absorbed a large amount of hydrogen compared with the unpolished plate, which suggests that thin oxide films on polished Ti would give poorer hydrogen barrier effects. Fig. 4(c) and 4(d) show the absorption properties of the irradiated plates with a fluence of 0.17 J cm^{-2} and 0.36 J cm^{-2}, respectively. The irradiation was performed on the unpolished plates because unpolished ones showed better hydrogen barrier effects, but did not show the perfect barrier effects. The plates irradiated at 0.17 J cm^{-2} and 0.36 J cm^{-2} had a metallic luster and were black, respectively. Compared with the unpolished plate, the amount of H_2 decreased for the plate irradiated with a fluence of 0.17 J cm^{-2}. However, the plate irradiated with a fluence of 0.36 J cm^{-2} absorbed a large amount of H_2. Fig. 5 shows the SEM images of the unpolished and polished plates after the hydrogen absorption tests. As shown in Fig. 5(a), it appeared that surface of the plate was covered with oxide films for the unpolished plate. On the

other hand, surface structures with cracks can be clearly shown for the polished plate in Fig. 5(b), suggesting that the oxide film is thin for the polished plate. As shown in the ref. [3], the rate-limiting factor for hydrogen absorption of Ti is the transport of hydrogen atoms through the oxide film, thus the thick oxide film of unpolished plate would result in the superior barrier effects compared with the thin film of the polished plate. Fig. 6 shows the SEM images, EDS spectra, and Raman spectra of the unpolished plate and irradiated plates after the hydrogen absorption tests. From the SEM end face observations, the plate irradiated with a fluence of 0.17 J cm^{-2} showed a film thickness of ~5 μm, indicated by the yellow arrows in Fig. 6(b). The film thickness of the plate irradiated with a fluence of 0.36 J cm^{-2} was greater than 15 μm as indicated by yellow arrows in Fig. 6(c). From the surface observations, the morphology changes of the plates are clearly observed. As shown in Fig. 6(d)–6(f), the unpolished Ti shows a morphology typical of a Ti plate, and the irradiated plates have surface films with micron-sized particles. It can be seen from the EDS spectra in Fig. 6(g) and 6(i) that only the oxygen amount increased with irradiation at 0.17 J cm^{-2} compared with unpolished Ti. However, the carbon and oxygen amounts increased with irradiation at 0.36 J cm^{-2} as shown in Fig. 6(k). Different chemical bonding states were detected from the Raman spectra in Fig. 6(h), 6(j), and 6(l). Although rutile TiO_2 peaks were observed for unpolished Ti, both anatase and rutile TiO_2 peaks were observed for the plate irradiated with a fluence of 0.17 J cm^{-2} [23]. Peaks corresponding to TiO_xC_y phases were observed for the plate irradiated with a fluence of 0.36 J cm^{-2} [24]. Therefore, the results showed that TiO_2 films can be grown with a fluence of 0.17 J cm^{-2} and TiO_xC_y films can be grown with a fluence of 0.36 J cm^{-2}. In order to analyze depth-dependent compositions, we performed the SEM-EDS analysis of the plate irradiated with 0.36 J cm^{-2} as shown in Fig. 7(a) and 7(b). From spot A to spot C, the ratio of C and O were similar, thus depth-dependent composition change in the TiO_xC_y film was not observed in the SEM-EDS. As shown in spot D for the bulk region, C and O was decreased compared with the film region. Fig. 7(c) and 7(d) shows the XPS spectra of the irradiated plates for Ti 2p and O 1s, respectively. The analysis was performed for the outermost surface of the plates. The Ti 2p spectra for both irradiated Ti plates were typical to TiO_2 phase [25]. In the O 1s spectra, the peaks at 529.9 eV corresponds to lattice oxygen of TiO_2. The peak at 531.6 eV for the 0.36 J cm^{-2} and the peak at 532.2 eV for the 0.17 J cm^{-2} would correspond to C-O and C=O species [25].

On the basis of above results, the TiO_xC_y phase was basically formed by the irradiation of Ti plates with a fluence of 0.36 J cm^{-2}. This phase was also formed for the irradiation of Ti powders

as shown in Section 3.1, but as shown in the SEM-EDS, oxygen amounts in the powders were smaller than those for in the plates. This difference could be ascribed to the thin oxide film thickness of powders and the difference of dissolved oxygen amounts. The powder samples were irradiated without exposure to air, but the plate samples were irradiated with exposure to air. The formation process of TiO_xC_y phase can be understood by the reduction of TiO_2 in the reductive gases formed by the decomposition of acetone by the high fluence irradiation. A previous study of unfocused YAG laser irradiation to CuO nanoparticles in acetone showed the formation of Cu_2O and Cu, and composition ratios of Cu_2O and Cu increased as the fluence increased [26]. Under a high fluence irradiation, acetone molecule on the irradiated powders would cause thermal decomposition and reductive gases (containing C and H) could reduce CuO in this system [26]. Thus, the similar reduction process into TiO_2 could form TiC_xO_y phase. If the further reduction proceeds, TiC phase also can be formed as shown in Fig. 2(a). In this study, the wavelength of the laser was 532 nm. In general, TiO_2 does not absorb visible light, thus the heat generation with the absorption of the laser would occur in metallic Ti just beneath the TiO_2 film, which would be also helpful to understand the formation process. The details of the process should be investigated further.

As shown in Fig. 4, the hydrogen absorption behavior of the unpolished Ti plate was similar to those of Ti plates irradiated with 0.17 J cm^{-2} and 0.36 J cm^{-2}. The irradiations were performed on the unpolished plates and thus these plates showed similar behaviors. The similar microstructures and surface chemical bonding states between the unpolished plate and the plate irradiated with 0.17 J cm^{-2} would result in the almost identical absorption behavior. On the other hands, the polished plate showed a large amount of absorption. This would be originated from the thin oxide film and cracks formation by the polishing. The causes of the poorer hydrogen barrier effects with irradiation at 0.36 J cm^{-2} are the irradiated microstructures. Although a film with dome-shaped particles was formed with a fluence of 0.36 J cm^{-2}, the film porosity was high compared with that of the film formed with a fluence of 0.17 J cm^{-2}. In addition, many cracks were generated by the shock waves of the YAG laser, as shown in Fig. 6(c). Thus, considering these microstructure features, irradiation with a low fluence would be better for the barrier coating. In this study, a small amount of hydrogen was absorbed by the plate formed with a fluence of 0.17 J cm^{-2}. To prevent hydrogen absorption by Ti plates completely, it could be promising to perform laser irradiation of the plate end faces and form thick surface films by increasing the pulse number. Additionally, a

composite coating should be considered for the synthesis of practical hydrogen barrier coatings [27]. In this study, facile pulsed laser coating of Ti plates was performed with different fluences, and the hydrogen absorption properties and microstructures of the coatings were investigated.

4. Conclusions

In this study, nanosecond pulsed laser irradiation was performed on Ti powders in acetone with no collective lens. Under a fluence of 0.36 J cm^{-2}, carbon was introduced on the Ti surfaces, and TiO_xC_y films were formed. The hydrogen absorption temperatures were slightly increased by the laser irradiation. After one activation cycle of hydrogen absorption and desorption, the hydrogen reabsorption temperature of non-irradiated Ti powders was low at ~167 °C. However, the laser-irradiated powders absorbed hydrogen above 260 °C. Thus, TiO_xC_y films show hydrogen barrier effects. For coating Ti plates as structural materials, pulsed laser irradiation was also performed on Ti plates in acetone. Hydrogen absorption by Ti plates requires a high temperature above 500 °C, which is higher than the absorption temperature of the powders. The TiO_xC_y film coatings on the Ti plates irradiated with the same fluence as the powders (0.36 J cm^{-2}) had a large amount of hydrogen absorption compared with the non-irradiated unpolished Ti plate. The change in chemical bonding state, high porosity of the coating films, and crack formation by shock waves result in poorer properties. Under irradiation at a low fluence of of 0.17 J cm^{-2}, TiO_2 films can be grown instead of TiO_xC_y films, and these films resulted in improved hydrogen barrier effects. The chemical bonding states of the surface films can be controlled by the laser fluence. This fundamental study would be helpful for understanding the hydrogen absorption process of Ti, and for developing hydrogen barrier coatings using a nanosecond pulsed laser.

CRediT authorship contribution statement

Yuki Nakagawa: Conceptualization, Funding acquisition, Investigation, Writing – original draft. **Genki Sugimoto:** Investigation, Visualization. **Tamaki Shibayama:** Supervision, Writing – review & editing.

Declaration of competing interest

The authors declare that they have no known competing financial interests or personal relationships that could have appeared to influence the work reported in this paper.

Data availability

Data will be made available on request.

Acknowledgments

This work was supported by JSPS KAKENHI grant number 21K14453. Part of this work was supported by "Advanced Research Infrastructure for Materials and Nanotechnology in Japan (ARIM)" of the Ministry of Education, Culture, Sports, Science and Technology (MEXT), grant numbers JPMXP1223HK0022 and JPMXP1224HK0013 (Hokkaido University). The authors are thankful to Keita Suzuki for his help in the XPS experiments. We thank Heather Fish, MChem from Edanz (https://jp.edanz.com.ac) for editing a draft of this manuscript.

References

[1] W.E. Wang, Thermodynamic evaluation of the titanium-hydrogen system, J. Alloys Compd. 238 (1996) 6-12. https://doi.org/10.1016/0925-8388(96)02264-5.

[2] Y. Hirooka, M. Miyake, T. Sano, A study of hydrogen absorption and desorption by titanium, J. Nucl. Mater. 96 (1981) 227-232. https://doi.org/10.1016/0022-3115(81)90566-3.

[3] E. Hadjixenophontos, L. Michalek, M. Roussel, M. Hirscher, G. Shimitz, The role of surface oxides on hydrogen sorption kinetics in titanium thin films, Appl. Surf. Sci. 441 (2018) 324-330. https://doi.org/10.1016/j.apsusc.2018.02.044.

[4] K. Shinzato, S. Hamamoto, H. Miyaoka, T. Ichikawa, Room-Temperature Hydrogen Absorption of Titanium with Surface Modification by Organic Solvents, J. Phys. Chem. C 123 (2019) 19269-19274. https://doi.org/10.1021/acs.jpcc.9b02014.

[5] K. Shinzato, Y. Nakagawa, S. Hamamoto, Y. Hayashi, H. Miyaoka, S. Isobe, T. Shibayama, N. Ogita, T. Ichikawa, Surface modification effects of graphite for selective hydrogen absorption by titanium at room temperature, Chem. Commun. 56 (2020) 7237-7240. https://doi.org/10.1039/D0CC03023F.

[6] K. Shinzato, Y. Nakagawa, S. Yang, S. Isobe, T. Shibayama, H. Miyaoka, T. Ichikawa, Room-Temperature Hydrogen Absorption of Ti with Robust Surface Coated by Hexagonal Boron Nitride, ACS Appl. Energy Mater. 5 (2022) 951-957. https://doi.org/10.1021/acsaem.1c03348.

[7] I. Wyrebska, K. Tomczyk, D. Siemiaszko, D. Zasada, J.D. Wojcik, M. Peska, R. Chulist, S. Koter, M. Polanski, Spontaneous room temperature reaction of titanium and its alloys with hydrogen during self-shearing reactive milling, Chem. Eng. J. 485 (2024) 149673. https://doi.org/10.1016/j.cej.2024.149673.

[8] R. Kondo, Y. Myokai, Y. Obora, H.T. Takeshita, Surface Structures and Hydrogenation Properties of Ti-Pd Alloys Immersed in Hydrogen Peroxide, Mater. Trans. 64 (2023) 2615-2621. https://doi.org/10.2320/matertrans.mt-m2023089.

[9] Y. Li, F. Barzagli, P. Liu, X. Zhang, Z. Yang, M. Xiao, Y. Huang, X. Luo, C. Li, H. Luo, R. Zhang, Mechanism and Evaluation of Hydrogen Permeation Barriers: A Critical Review, Ind. Eng. Chem. Res. 62 (2023) 15752-15773. https://doi.org/10.1021/acs.iecr.3c02259.

[10] M. Wetegrove, M.J. Duarte, K. Taube, M. Rohloff, H. Gopalan, C. Scheu, G. Dehm, A. Kruth, Preventing Hydrogen Embrittlement: The Role of Barrier Coatings for the Hydrogen Economy, Hydrogen 4 (2023) 307-322. https://doi.org/10.3390/hydrogen4020022.

[11] S. Xiao, X. Meng, K. Shi, L. Liu, H. Wu, W. Lian, C. Zhou, Y. Lyu, P.K. Chu, Hydrogen permeation barriers and preparation techniques: A review, J. Vac. Sci. Technol. A 40 (2022) 060803. https://doi.org/10.1116/6.0002178.

[12] T. Leguey, N. Baluc, F. Jansen, M. Victoria, Characterization of hydrogen barrier coatings for titanium-base alloys, J. Nucl. Mater. 307-311 (2002) 1329-1333. https://doi.org/10.1016/S0022-3115(02)01297-7.

[13] J. Tao, X. Guo, Z. Huang, H. Liu, T. Wang, Preparation and characterization of enamel coating on pure titanium as a hydrogen penetration barrier, Nucl. Eng. Des. 259 (2013) 65-70. https://doi.org/10.1016/j.nucengdes.2013.02.041.

[14] T. Kim, J. Lee, S. Kim, E. Hong, H. Lee, Hydrogen permeation barrier of carbon-doped TiZrN coatings by laser carburization, Corros. Sci. 190 (2021) 109700. https://doi.org/10.1016/j.corsci.2021.109700.

[15] B.F. Mohazzab, B. Jaleh, O. Kakuee, A. Fattah-alhosseini, Formation of titanium carbide on the titanium surface using laser ablation in n-heptane and investigating its corrosion resistance, Appl. Surf. Sci. 478 (2019) 623-635. https://doi.org/10.1016/j.apsusc.2019.01.259.

[16] A. Bonis, A. Santagata, A. Galasso, A. Laurita, R. Teghil, Formation of Titanium Carbide (TiC) and TiC@C core-shell nanostructures by ultra-short laser ablation of titanium carbide

and metallic titanium in liquid, J. Colloid Interf. Sci. 489 (2017) 76-84. https://doi.org/10.1016/j.jcis.2016.08.078.

[17] Y. Ishikawa, T. Tsuji, S. Sakaki, N. Koshizaki, Pulsed laser melting in liquid for crystalline spherical submicrometer particle fabrication- Mechanism, process control, and applications, Prog. Mater. Sci. 131 (2023) 101004. https://doi.org/10.1016/j.pmatsci.2022.101004.

[18] G. Greczynski, L. Hultman, Reliable determination of chemical state in x-ray photoelectron spectroscopy based on sample-work-function referencing to adventitious carbon: resolving the myth of apparent constant binding energy of the C 1s peak, Appl. Surf. Sci. 451 (2018) 99-103. https://doi.org/10.1016/j. apsusc.2018.04.226.

[19] V. Mansfeldova, M. Zlamalova, H. Tarabkova, P. Janda, M. Vorokhta, L. Piliai, L. Kavan, Work Function of TiO_2 (Anatase, Rutile, and Brookite) Single Crystals: Effects of the Environment, J. Phys. Chem. C 125 (2021) 1902-1912. https://doi.org/10.1021/acs.jpcc.0c10519.

[20] K. Shinzato, Study on Hydrogen Absorption Properties of Titanium with Surface Modification, Ph.D dissertation of Hiroshima University (2020). https://ir.lib.hiroshima-u.ac.jp/00050362.

[21] J.C. Stotts, R. Salehin, I.N. Bakst, G.B. Thompson, C.R. Weinberger, Hydrogen diffusion and storage in substoichiometric TiC, Int. J. Hydrogen Energy 50 (2024) 512-523. https://doi.org/10.1016/j.ijhydene.2023.07.264.

[22] H. Ding, X. Fan, C. Li, X. Liu, D. Jiang, C. Wang, First-principles study of hydrogen storage in non-stoichiometric TiC_x, J. Alloys Compd. 551 (2013) 67-71. https://doi.org/10.1016/j.jallcom.2012.10.067.

[23] S. Challagulla, K. Tarafder, R. Genesan, S. Roy, Structure sensitive photocatalytic reduction of nitroarenes over TiO_2, Sci. Rep. 7 (2017) 8783. https://doi.org/10.1038/s41598-017-08599-2.

[24] C. Rudiger, M. Favaro, C.V. Vidal. L. Calvillo, N. Bozzolo, S. Jacomet, J. Hein, L. Gregoratti, S. Agnoli, G. Granozzi, J.K. Liebhauser, Substrate Grain-Dependent Chemistry of Carburized Planar Anodic TiO_2 on Polycrystalline Ti, ACS Omega 2 (2017) 631-640. https://doi.org/10.1021/acsomega.6b00472.

[25] G. Greczynski, L. Hultman, X-ray photoelectron spectroscopy: Towards reliable binding energy referencing, Prog. Mater. Sci. 107 (2020) 100591. https://doi.org/10.1016/j.pmatsci.2019.100591.

[26] H. Wang, A. Pyatenko, K. Kawaguchi, X, Li, Z. Swiatkowska-Warkocka, N. Koshizaki, Selective Pulsed Heating for the Synthesis of Semiconductor and Metal Submicrometer Spheres, Angew. Chem. Int. Ed. 49 (2010) 6361-6364. https://doi.org/10.1002/anie.201002963.

[27] Z. Lu, Q. Zhou, Y. Ling, B. Hou, J. Wang, Z. Zhang, Preparation and hydrogen penetration performance of TiO_2/TiC_x composite coatings, Int. J. Hydrogen Energy 45 (2020) 14048-14061. https://doi.org/10.1016/j.ijhydene.2020.03.049.

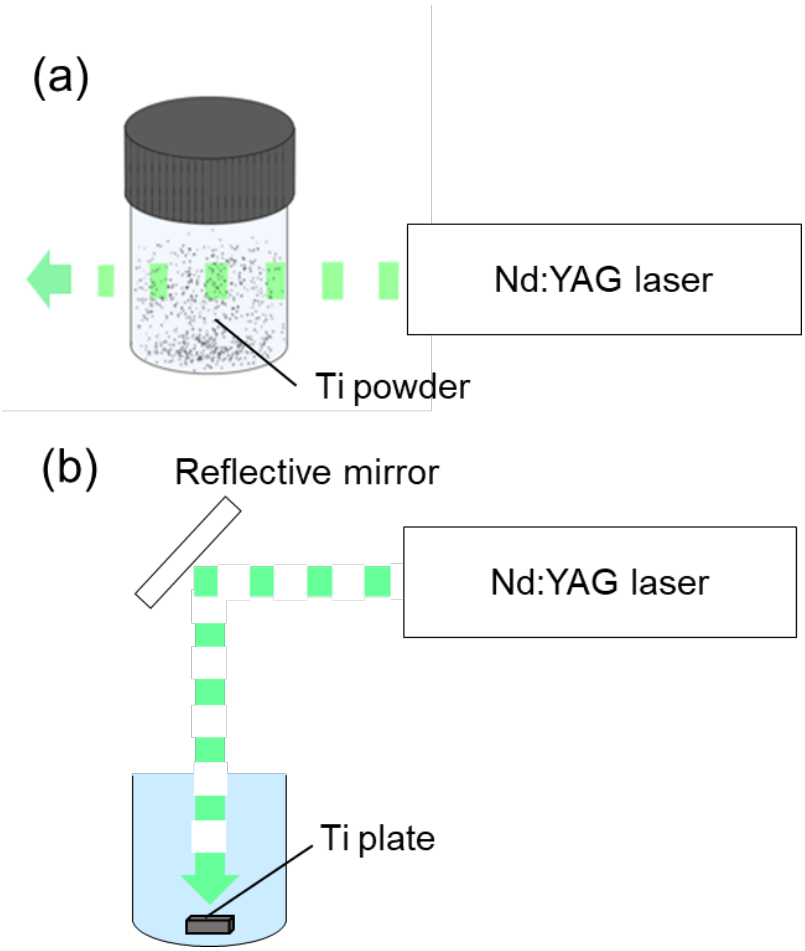

Fig. 1 The experimental setups for the laser irradiation experiments: (a) Ti powders and (b) Ti plates.

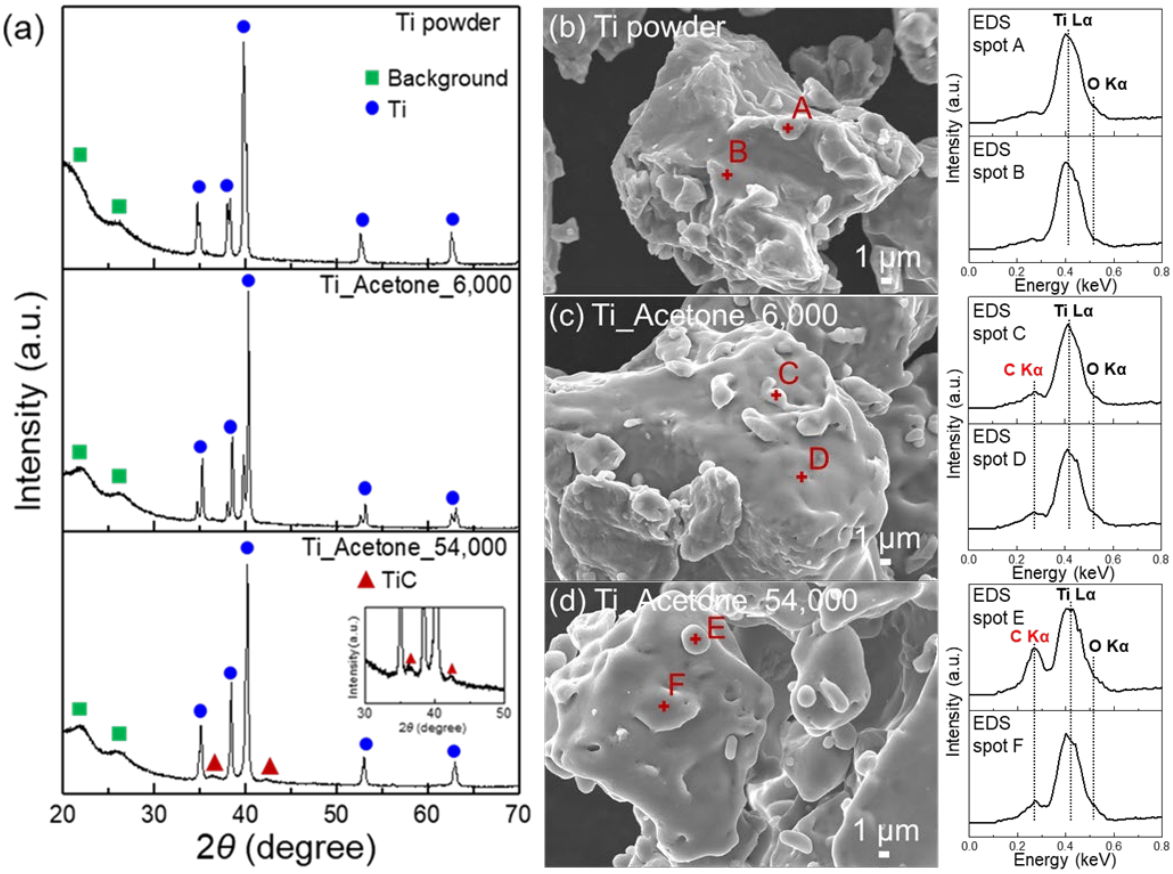

Fig. 2 (a) XRD profiles of pristine Ti powders and irradiated powders, (b) SEM image and EDS spectra from spot A and B for pristine Ti powders, (c) SEM image and EDS spectra from spot C and D for Ti powders irradiated with 6000 pulses, and (d) SEM image and EDS spectra from spot E and F for Ti powders irradiated with 54,000 pulses. The laser fluence was 0.36 J cm^{-2}.

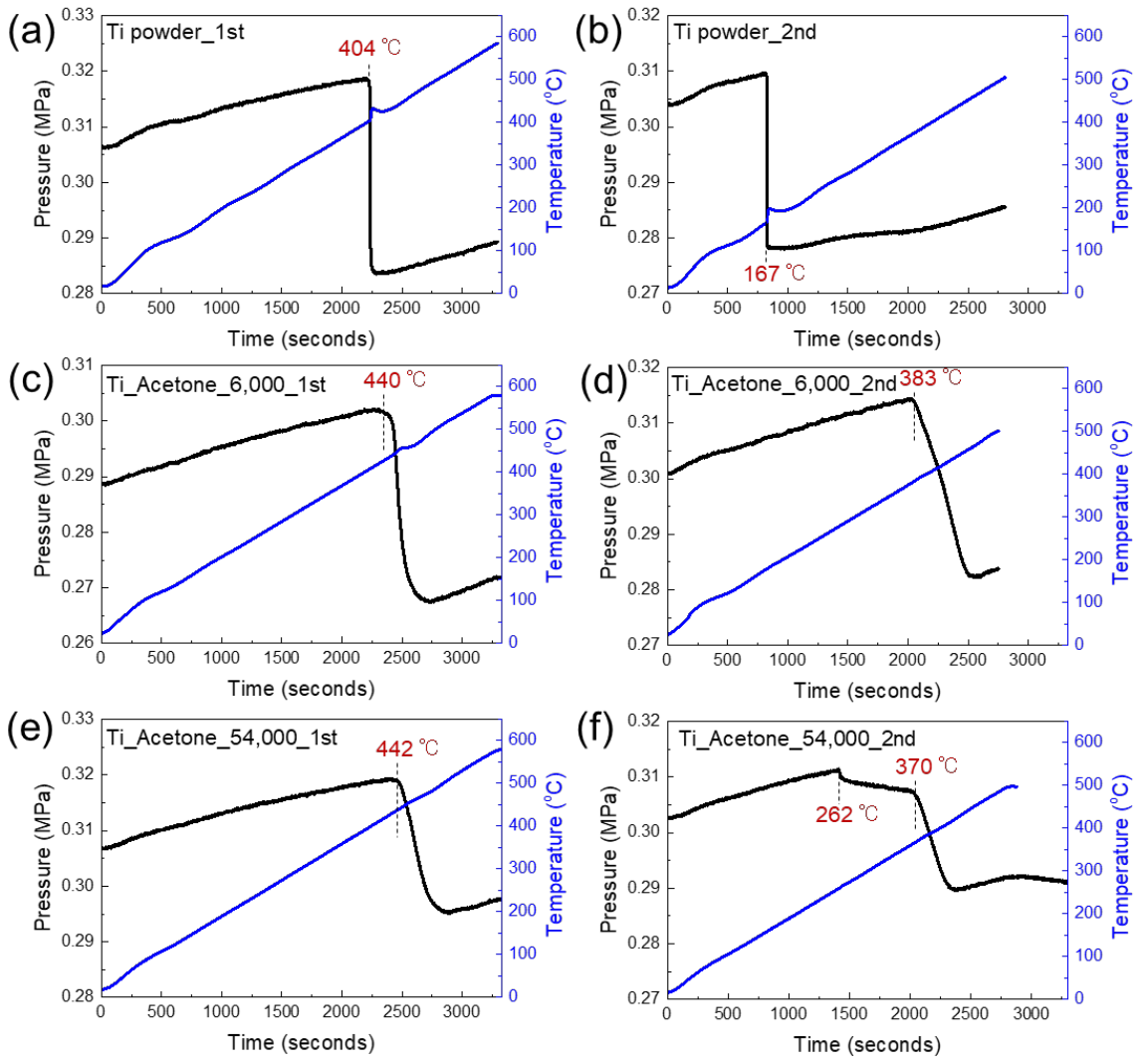

Fig. 3 Hydrogen absorption properties of (a and b) pristine Ti powders, (c and d) Ti powders irradiated with 6000 pulses, and (e and f) Ti powders irradiated with 54,000 pulses. The laser fluence was 0.36 J cm^{-2}. The first absorption properties and second absorption properties after the activation treatments are shown in (a, c, e) and (b, d, f), respectively.

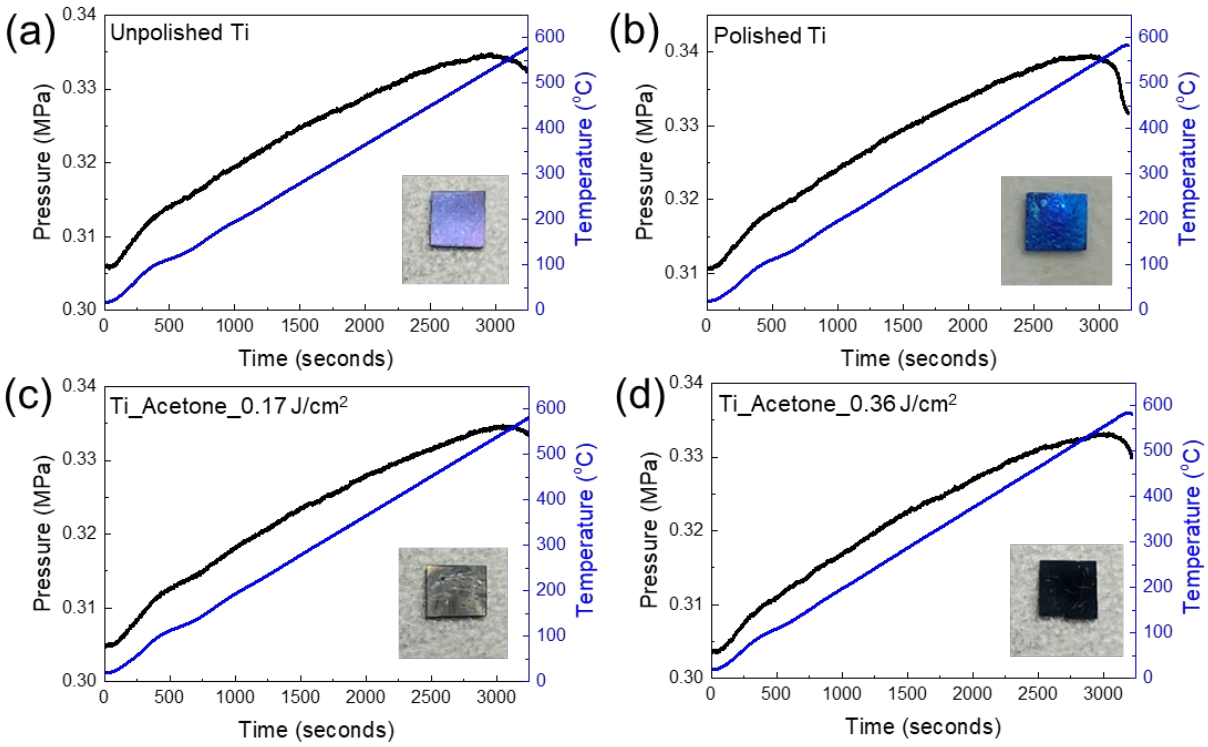

Fig. 4 Hydrogen absorption properties of the (a) unpolished Ti plate, (b) polished Ti plate, (c) unpolished Ti plate irradiated with a fluence of 0.17 J cm^{-2}, and (d) unpolished Ti plate irradiated with a fluence of 0.36 J cm^{-2}. For (c) and (d), irradiation with 18,000 pulses was performed on both the front and back sides. The insets show a picture of the Ti plate after the hydrogen absorption test. The length of each Ti plate was ~4 mm.

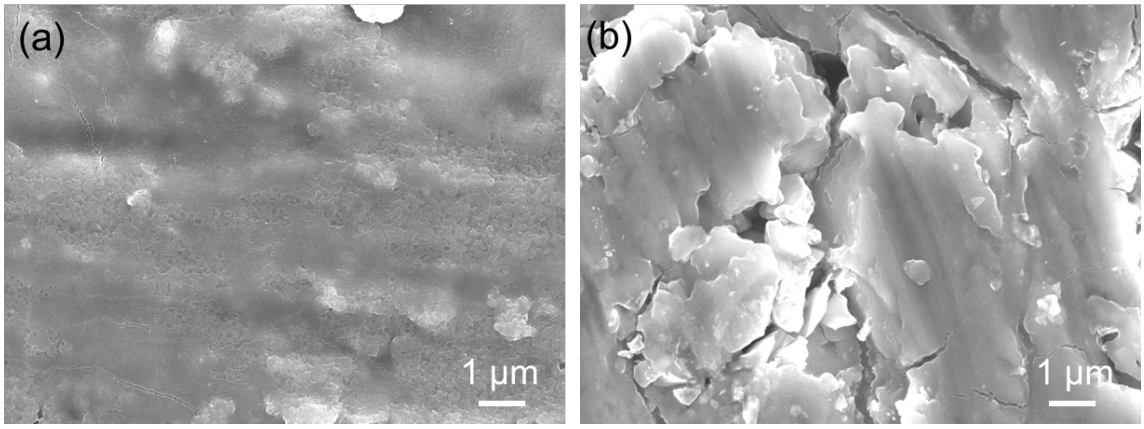

Fig. 5 SEM images of the surfaces of Ti plates after hydrogen absorption tests: (a) unpolished plate and (b) polished plate. The unpolished plate

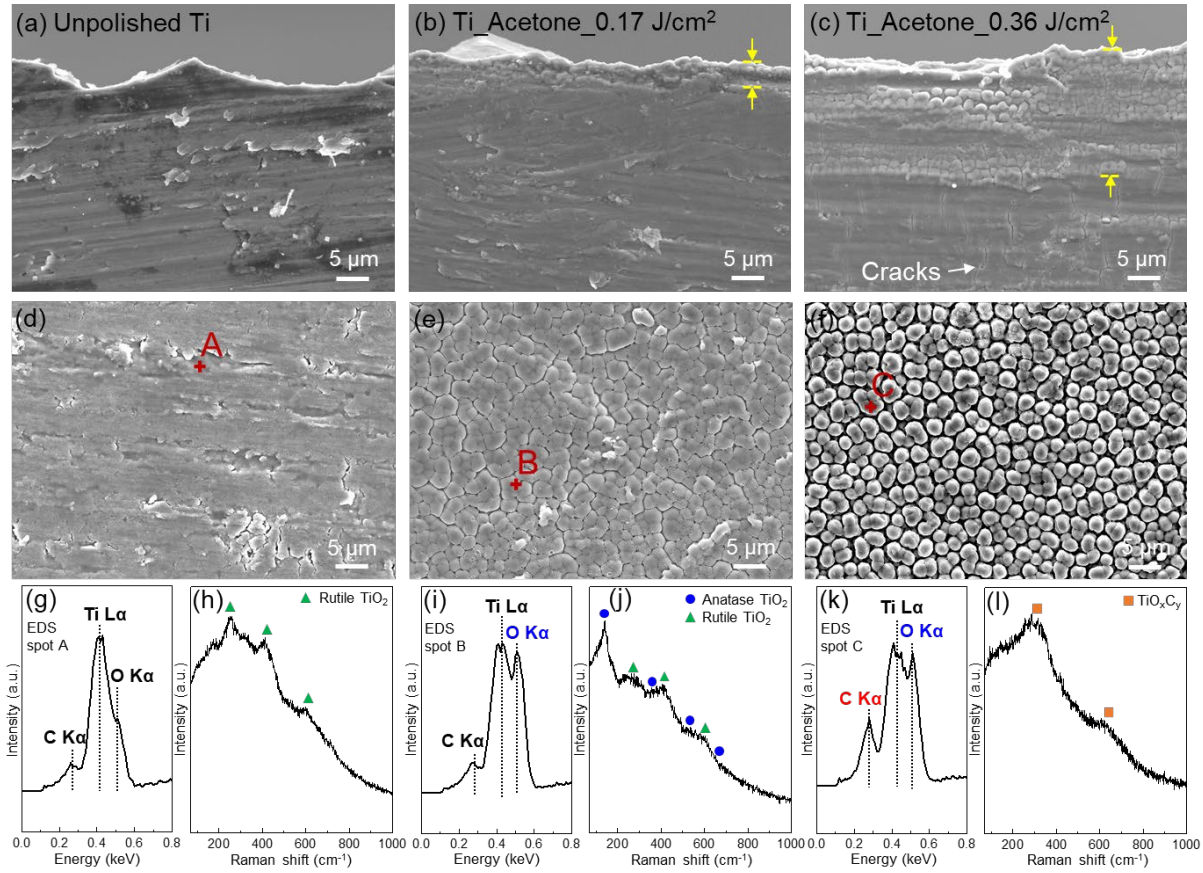

433

434 Fig. 6 Microstructures and chemical bonding states of the surface films of unpolished and
435 irradiated Ti plates after hydrogen absorption tests: (a–c) SEM images of the end faces of Ti plates,
436 (d–f) SEM images of the surfaces of Ti plates, (g, i, k) EDS spectra from spots A, B, and C, and
437 (h, j, l) Raman spectra of unpolished Ti, Ti irradiated with a fluence of 0.17 J cm^{-2}, and Ti
438 irradiated with a fluence of 0.36 J cm^{-2}.

439

440

441

442

443

444

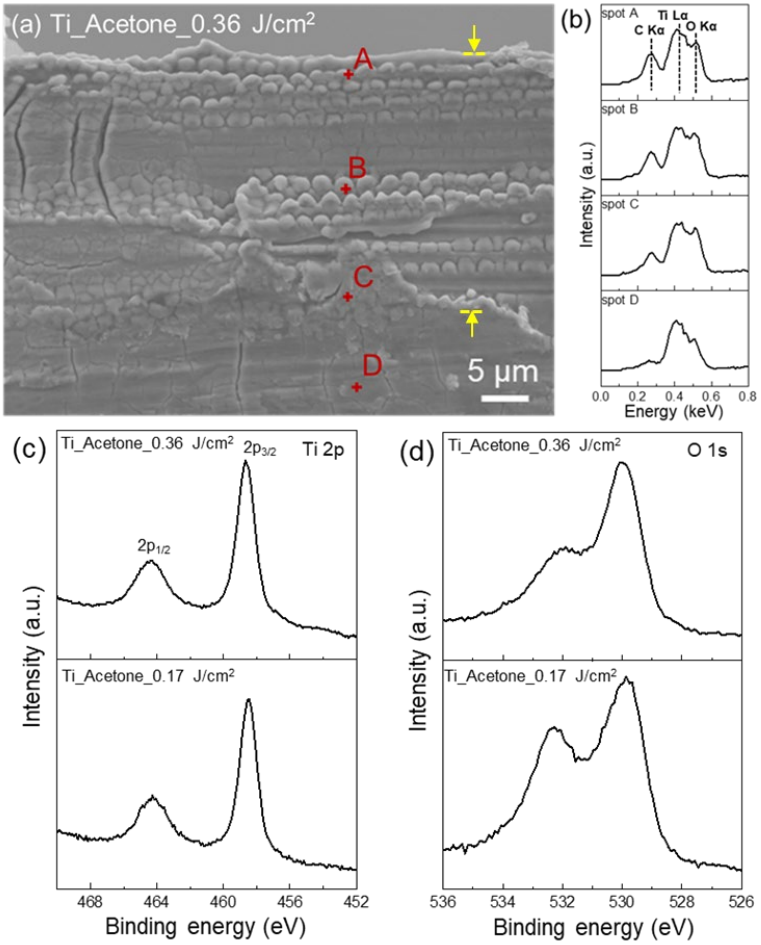

445

446 Fig. 7 (a) SEM image of end face of Ti irradiated with a fluence of 0.36 J cm^{-2}, (b) EDS spectra
447 from spots A, B, C, and D, (c) XPS Ti 2p spectra of Ti plates irradiated with a fluence of 0.36 J
448 cm^{-2} and 0.17 J cm^{-2}, and (d) XPS O 1s spectra of Ti plates irradiated with a fluence of 0.36 J
449 cm^{-2} and 0.17 J cm^{-2}.